Magnetic order of Dy in $DyBa_2Cu_3O_7$

T. W. Clinton and J. W. Lynn
Center for Superconductivity Research, Department of Physics, University of Maryland, College Park, Maryland 20742 and Reactor Division, National Institute of Standards and Technology, Gaithersburg, Maryland 20899

J. Z. Liu, Y. X. Jia, and R. N. Shelton
Department of Physics, University of California, Davis, California 95616

Neutron diffraction has been used to study the magnetic fluctuations and long range order of the Dy ions in single crystals of superconducting $DyBa_2Cu_3O_7$. The temperature dependence of the rod of scattering, characteristic of 2D behavior, has been measured above and below the 3D Néel temperature ($T_N \cong 0.9$ K). This rod intensity is observed to increase as the temperature decreases until T_N is reached, and then the intensity decreases rapidly below T_N. The 2D magnetic correlation length, which is obtained from measurements of the width of the rod, grows continuously with decreasing temperature, then reaches a resolution-limited maximum at the Néel temperature when long range magnetic order sets in. At low T, two separate types of simple 3D antiferromagnetic structures are found, one characterized by a wave vector of $(\frac{1}{2}\frac{1}{2}\ 0)$, and the other by $(\frac{1}{2}\frac{1}{2}\frac{1}{2})$. We believe the two types of order occur because the (dipolar) energies for these two configurations are nearly identical. This behavior is analogous to the 2D and 3D magnetic order of Er observed in $ErBa_2Cu_3O_7$.

The magnetic ordering of the rare-earth ions in the layered superconducting oxides has been of interest both because of the magnetic-superconductor interactions, and because of the 2D magnetic behavior these materials display.[1–5] In the $RBa_2Cu_3O_7$ (R = rare earth) materials of direct interest here, the 2D behavior originates naturally from the crystallography; there is only one rare-earth ion per chemical unit cell, and the c axis is three times as long as the a and b axes. Powder neutron diffraction experiments on $ErBa_2Cu_3O_7$ (Ref. 3) were the first to confirm two-dimensional behavior of the rare-earth ions in the $RBa_2Cu_3O_7$ system. Although the Er magnetic system is 2D in character, when strong 2D correlations develop in the a-b plane a weak interaction along the c axis induces three-dimensional long-range order at $T_N = 0.618$ K.[1,2] Despite the observed 2D nature of the magnetic ordering of Er in $ErBa_2Cu_3O_7$ and the expected 2D magnetic nature of all the rare-earth ions in $RBa_2Cu_3O_7$, only 3D long-range order has been seen in the other rare-earth systems Dy,[6] Nd,[7] and Gd.[8]

In this article we report measurements on a single crystal of $DyBa_2Cu_3O_7$. Above the 3D ordering temperature we observe a rod of scattering along $(\frac{1}{2}\frac{1}{2}\ Q_z)$, which directly demonstrates the 2D character of the system. In addition, the rod intensity, which is proportional to the magnetic susceptibility, rises to a peak at T_N. We have also studied the development of magnetic correlations in the a-b plane, which reach a maximum at the Néel temperature when long-range order sets in. At low T two separate 3D antiferromagnetic structures occur, with nearly identical (dipolar) energies; the $(\frac{1}{2}\frac{1}{2}\frac{1}{2})$ structure, corresponding to antiferromagnetically coupled spins along all three crystallographic directions, and the $(\frac{1}{2}\frac{1}{2}0)$ structure, which is antiferromagnetic along the a and b directions and ferromagnetic along c.

The neutron experiments were performed at the research reactor at the National Institute of Standards and Technology. The scattering data were taken with a wavelength of 2.3714 Å and a pyrolytic graphite monochromator and filter. A ^{3}He refrigerator was used for all the measurements. The growth technique for the single crystals has been described in a previous article.[1] The measured superconducting transition temperature for the crystal was $T_C \cong 90$ K. The crystal we used for our measurements weighed 2 mg.

To understand the observations on this system, consider first the scattering cross section[9]

$$\frac{d^2\sigma}{d\Omega_f dE_f} = \left(\frac{N}{\hbar}\right)\left(\frac{\gamma e^2}{mc^2}\right)^2\left(\frac{k_i}{k_f}\right)|f(\mathbf{Q})|^2 \times \sum_{ij}(\delta_{ij} - Q_iQ_j)S^{ij}(\mathbf{Q},\omega), \tag{1}$$

where $f(\mathbf{Q})$ is the magnetic form factor, $\mathbf{k}_i$ and $\mathbf{k}_f$ are the incoming and outgoing neutron wave vectors, respectively, and

$$S^{ij}(\mathbf{Q},\omega) = \frac{1}{2\pi}\int_{-\infty}^{\infty} e^{i(\mathbf{Q}\cdot\mathbf{r}-\omega t)}\sum_r \langle S^i(0,0)S^j(\mathbf{r},t)\rangle dt \tag{2}$$

is the space and time Fourier transform of the spin-spin correlation function of interest. For this discussion it is convenient to break the cross section into a Bragg and a diffuse part:

$$\left(\frac{d^2\sigma}{d\Omega_f dE_f}\right)_{\text{Bragg}} = \left(\frac{N}{\hbar}\right)\left(\frac{\gamma e^2}{mc^2}\right)^2|f(\mathbf{Q})|^2 \times \sum_{ij}(\delta_{ij} - Q_iQ_j) \times \delta(\omega)\langle S^i(-\mathbf{Q})\rangle\langle S^j(\mathbf{Q})\rangle \tag{3}$$

and

 0021-8979/91/105751-03$03.00

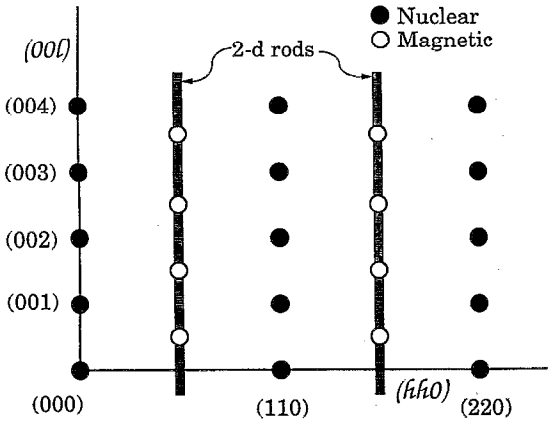

FIG. 1. The scattering plane in reciprocal space showing the positions of 3D nuclear and magnetic Bragg points as well as the 2D magnetic Bragg rods.

$$\left(\frac{d^2\sigma}{d\Omega_f dE_f}\right)_{\text{diffuse}} = \left(\frac{N}{\hbar}\right)\left(\frac{\gamma e^2}{mc^2}\right)^2\left(\frac{k_i}{k_f}\right)|f(\mathbf{Q})|^2 \times \sum_{ij}(\delta_{ij}-Q_iQ_j)\frac{1}{2\pi}\int_{-\infty}^{\infty} e^{i\omega t} \times [\langle S^i(-\mathbf{Q},0)S^j(\mathbf{Q},t)\rangle - \langle S^i(-\mathbf{Q},0)\rangle\langle S^j(\mathbf{Q},t)\rangle]dt. \quad (4)$$

Below T_N long-range order has set in, and Eq. (3) is a direct measure of the thermodynamic order parameter. The diffuse scattering in Eq. (4) tends to zero upon lowering the temperature below T_N, as it originates from low energy magnetic excitations. Thus, when long-range order sets in we see that the scattering intensity in Eq. (1) is proportional to the square of the sublattice magnetization. In the 3D case the scattering will peak about a magnetic reciprocal lattice vector and the scattering intensity will be in the form of magnetic Bragg peaks, as shown in Fig. 1.

Above T_N only short range correlations exist, and thus only the diffusive part will contribute to the scattering intensity in Eq. (1). For the present case where the neutron energy is much larger than the thermal fluctuations, the quasielastic approximation is well obeyed, and the cross section is proportional to the wave-vector dependent susceptibility $\chi^{ij}(\mathbf{Q})$.[10] Then Eq. (4) can be written as

$$\left(\frac{d\sigma}{d\Omega_f}\right)_{\text{diffuse}} = \int dE_f \left(\frac{d^2\sigma}{d\Omega_f dE_f}\right)_{\text{diffuse}} = \left(\frac{N}{\hbar}\right)\left(\frac{\gamma e^2}{mc^2}\right)^2\left(\frac{k_i}{k_f}\right)|f(\mathbf{Q})|^2 \times \left(\frac{k_B T}{g^2\mu_B^2}\right)\sum_{ij}(\delta_{ij}-Q_iQ_j)\chi^{ij}(\mathbf{Q}). \quad (5)$$

For a 2D system in the Ornstein–Zernike approximation we have

$$\chi^{ij}(\mathbf{Q}) \propto (\kappa^2 + Q_x^2 + Q_y^2)^{-1}, \quad (6)$$

and we can write

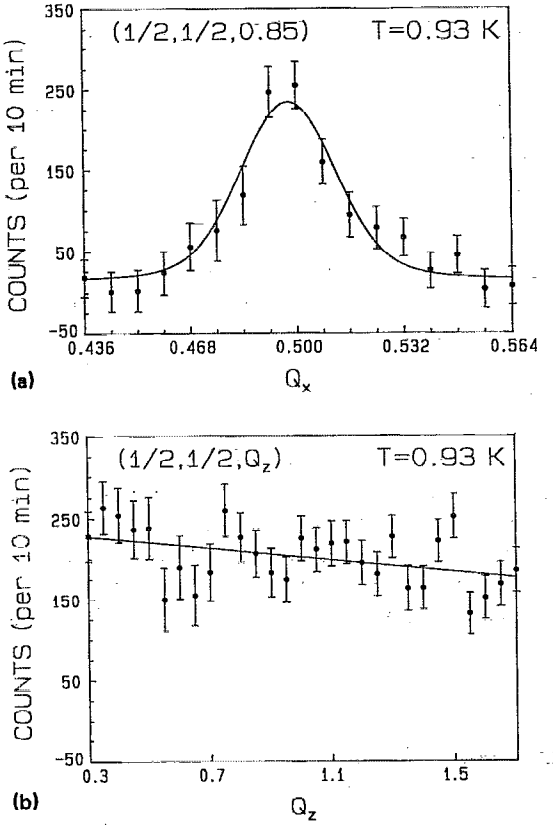

FIG. 2. (a) A scan across the rod of scattering in reciprocal space, showing the 2D character just above $T_N \cong 0.91$ K and (b) a scan along the rod, showing that the scattering intensity does not vary significantly along Q_z. Hence there are no significant spin correlations between planes, even just above T_N. The slight decrease in intensity with increasing Q_z is due to the magnetic form factor.

$$\left(\frac{d\sigma}{d\Omega_f}\right)_{\text{diffuse}} \propto \chi(\mathbf{Q}) \propto (\kappa^2 + Q_x^2 + Q_y^2)^{-1}, \quad (7)$$

where κ is the inverse correlation length within the a-b plane. Thus, in a 2D system we expect to see critical scattering about the reciprocal lattice positions as in the 3D case, with the important difference that in the 2D case the critical scattering should be independent of Q_z, so one should see a rod of scattering extending along Q_z.

In Fig. 1 we present a diagram of reciprocal space, showing the positions of the 3D nuclear (crystal structure) and magnetic (spin structure) Bragg points, as well as the Bragg rods associated with 2D character. Above the ordering temperature the rod intensity is due to short-range magnetic fluctuations in the a-b plane, while below T_N it arises from low energy magnetic excitations. Figure 2(a) shows a scan across the rod, just above the 3D ordering temperature. This strong rod of scattering develops for temperatures $\lesssim 2$ K. The linewidth of this peak is a measure of the inverse 2D correlation length κ as defined in Eq. (7). Thus, by scanning across the rod at various temperatures we have observed the evolution of the magnetic correlations in the a-b plane. Also shown in this figure is a scan along the rod, which demonstrates that the scattering intensity is independent of Q_z. Hence there are no signifi-

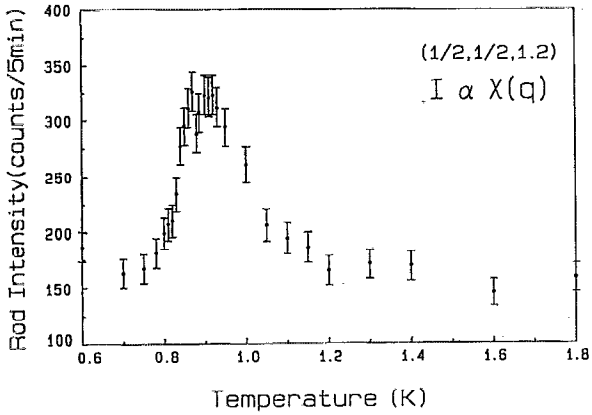

FIG. 3. Rod intensity as a function of temperature. The intensity is seen to peak at two temperatures, 0.91 and 0.87 K, which correspond to the approximate T_N's of the two different magnetic structures observed [$(\frac{1}{2}\frac{1}{2}\frac{1}{2})$ and $(\frac{1}{2}\frac{1}{2}0)$, respectively].

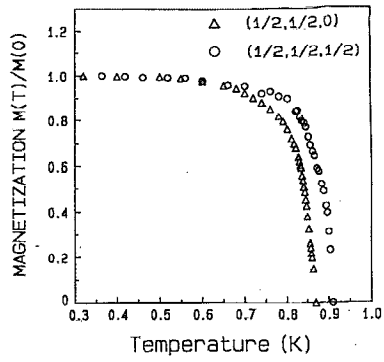

FIG. 4. Sublattice magnetization vs temperature obtained from the $(\frac{1}{2}\frac{1}{2}\frac{1}{2})$ 3D magnetic Bragg peak, with $T_N \cong 0.91$ K, contrasted with the data obtained from the $(\frac{1}{2}\frac{1}{2}0)$ peak, where $T_N \cong 0.87$ K.

cant correlations between spins in adjacent a-b planes, even though we are just above T_N. Therefore, above T_N the system only exhibits 2D short-range magnetic order.

Figure 3 shows the intensity at a point on the rod $(\frac{1}{2}\frac{1}{2}1.2)$ versus temperature. The rod starts to develop below about 2 K, and the intensity steadily increases with decreasing temperature until it peaks at T_N, when long-range order sets in. The two peaks in the rod intensity at $T \cong 0.91$ and 0.87 K are due to the two different Néel temperatures for the $(\frac{1}{2}\frac{1}{2}\frac{1}{2})$ and $(\frac{1}{2}\frac{1}{2}0)$ magnetic structures, respectively. Below T_N the intensity quickly decreases, presumably due to the sharp increase in the energy of the magnetic excitations, and the consequent decrease in their thermal population.

Next, we turn to the temperature dependence of the order parameter, Fig. 4, which is obtained from the 3D Bragg peaks $(\frac{1}{2}\frac{1}{2}\frac{1}{2})$ and $(\frac{11}{22}0)$, where the ordering temperatures are about 0.91 and 0.87 K, respectively. Both curves are quite sharp, a characteristic of the expected 2D Ising behavior as found for the $ErBa_2Cu_3O_7$ system,[1] although in this crystal there is a distribution of transition temperatures that appears to spoil quantitative agreement. The 3D ordering is simply being induced as a necessary consequence of the onset of long-range order within the a-b planes.[10] This behavior is analogous to the 2D and 3D magnetic ordering of Er observed in $ErBa_2Cu_3O_7$.[1,2]

Research at Maryland is supported by the NSF, DMR 89-21878. Research at U. C. Davis was performed under the auspices of the U. S. Department of Energy for Lawrence Livermore National Laboratory under Contract No. W-7405-ENG-48.

Note added in proof. More recently we further annealed the sample in oxygen and repeated our measurements. The annealing of the Dy123 crystal eliminated the whole-integral magnetic Bragg peaks $(\frac{1}{2}\frac{1}{2}l)$, and we also observed a slight increase in T_N associated with the half integral peaks $(\frac{1}{2}\frac{1}{2}l/2)$. In addition, we made measurements on an oxygen deficient sample in which we only observed whole integral magnetic peaks $(\frac{1}{2}\frac{1}{2}l)$ as well as a lowering of T_N. Thus, we conclude that the $(\frac{1}{2}\frac{1}{2}l/2)$ peaks, corresponding to antiparallel spins along the a, b and c axes, represent the correct magnetic structure for the fully oxygenated sample, and as oxygen is removed T_N is lowered and the structure changes to $(\frac{1}{2}\frac{1}{2}l)$, corresponding to parallel spins along the c axis.

[1] J. W. Lynn, T. W. Clinton, W-H. Li, R. W. Erwin, J. Z. Liu, K. Vandervoort, and R. N. Shelton, Phys. Rev. Lett. **63**, 2606 (1989).
[2] J. W. Lynn, T. W. Clinton, W-H. Li, R. W. Erwin, J. Z. Liu, R. N. Shelton, and P. Klavins, J. Appl. Phys. **67**, 4533 (1990).
[3] J. W. Lynn, W-H. Li, Q. Li, H. C. Ku, H. D. Yang, and R. N. Shelton, Phys. Rev. B **36**, 2374 (1987).
[4] H. Zhang, J. W. Lynn, W-H. Li, T. W. Clinton, and D. E. Morris, Phys. Rev. B **41**, 11 229 (1990).
[5] A recent review of the oxide superconductors is given in *High Temperature Superconductivity*, edited by J. W. Lynn (Springer, New York, 1990).
[6] A. I. Goldman, B. X. Yang, J. Tranquada, J. E. Crow, and C-S. Jee, Phys. Rev. B **36**, 7234 (1987); P. Fischer, K. Kakurai, M. Steiner, K. N. Clausen, B. Lebechi, F. Hulliger, H. R. Ott, P. Brüesch, and P. Unternahrer, Physica C **152**, 145 (1988).
[7] K. N. Yang, J. M. Ferreira, B. W. Lee, M. B. Maple, W-H. Li, J. W. Lynn, and R. W. Erwin, Phys. Rev. B **40**, 10 963 (1989).
[8] D. McK. Paul, H. A. Mook, A. W. Hewit, B. C. Sales, L. A. Boatner, J. R. Thompson, and M. Mostoller, Phys. Rev. B **37**, 2341 (1988).
[9] S. W. Lovesey, *Theory of Neutron Scattering from Condensed Matter* (Oxford, New York, 1984), Vol. 2.
[10] R. J. Birgeneau, H. J. Guggenheim, and G. Shirane, Phys. Rev. B **1**, 2211 (1970).